Power Engineering and Engineering Thermophysics
https://www.acadlore.com/journals/PEET

Numerical Analysis of Heat Transfer Enhancement Using Fe_3O_4 Nanofluid Under Variable Magnetic Fields

Asaad Abdulnabi Lazim[1], Alireza Daneh-Dezfuli[1], Laith Jaafer Habeeb[2*]

[1] Mechanical Engineering Department, Faculty of Engineering, Shahid Chamran University of Ahvaz, 61xxx Ahvaz, Iran
[2] Training and Workshop Center, University of Technology- Iraq, 10001 Baghdad, Iraq

* Correspondence: Laith Jaafer Habeeb (Laith.J.Habeeb@uotechnology.edu.iq)

Received: 12-03-2023 **Revised:** 01-20-2024 **Accepted:** 01-26-2024

Citation: A. A. Lazim, A. Daneh-Dezfuli, and L. J. Habeeb, "Numerical analysis of heat transfer enhancement using Fe_3O_4 nanofluid under variable magnetic fields," *Power Eng. Eng. Thermophys.*, vol. 3, no. 1, pp. 1–11, 2024. https://doi.org/10.56578/peet030101.

Abstract: This study conducts a numerical investigation into the heat transfer enhancement of Fe_3O_4-distilled water nanofluid within a magnetically influenced environment. The research is centered on the analysis of the impact of varying magnetic field strengths on the heat transfer characteristics in a controlled tube setting. The tube, possessing an inner diameter of 25.4 mm and a length of 210 mm, serves as the medium for the flow of nanofluid, initially at 300 K. The influence of magnetism on the nanofluid's thermal boundary layer and the formation of fluid vortices is meticulously examined, leveraging the application of magnetic fields ranging from one to three Teslas. In this context, the study observes the behavior of magnetic particles under these fields, revealing their attraction or repulsion, subsequently inducing turbulence and modifying flow patterns. It is noted that increased flow velocities tend to shield the magnetic field's thermal effects. A key focus is placed on the Nusselt number and Y^+ as indicators of heat transfer efficiency, both of which demonstrate significant variations with changes in the magnetic field strength and fluid velocity. The Nusselt number, in particular, escalates to a peak value of 128.7 when exposed to a 0.1 m/s flow velocity and a magnetic field of 3 Teslas. The findings suggest an interrelation between increased magnetic field strengths and the entrance of the fluid into a turbulent state, thereby facilitating an efficient temperature transfer to the fluid. Notably, this research sheds light on the prospect of using ferrofluid-based cooling systems in electrical equipment, highlighting the potential of magnetically manipulated nanofluids to enhance heat transfer capabilities. The investigation delineates how the interplay between magnetic fields, fluid velocity, and nanofluid properties can be optimized for improved thermal management in various applications.

Keywords: Fluid vortex; Magnetic field; Numerical simulation; Inlet velocity; Heat transfer enhancement

1 Introduction

This review meticulously examines key research areas in internal forced convection flow, emphasizing both experimental and theoretical studies. Ferrofluids, comprising magnetic nanoparticles suspended in a carrier liquid, are instrumental in diverse applications including drug delivery, fluid pumping, heat transport, and cancer treatment. These fluids respond to changes in magnetic fields, temperature, and density, thereby influencing convection and modifying the distribution of body forces in fluids. Common carrier liquids include oils, kerosene, and water [1]. Ferrofluids are colloidal dispersions of magnetic particles, typically sized between 5–15 nm, and are coated with surfactants to prevent aggregation. Despite their nomenclature, ferrofluids are not ferromagnetic but exhibit paramagnetic properties [2]. The predominant method for nanofluid production is a two-step process. Initially, nanoscale materials with desired thermal and rheological properties are generated through physical or chemical processes. Subsequently, these nanoparticles are dispersed in the base fluid using vigorous mixing techniques such as high-shear stirring, ball milling, ultrasonic probe sonication, or magnetic agitation. The two-step method is favored for its simplicity and cost-effectiveness. However, it presents challenges, notably the tendency of particles to aggregate. The application of surfactants reduces surface tension in the base fluid and enhances nanofluid dispersion stability. This method, while widely used, has limitations, including a narrow range of effective magnetic field strengths [3–6], with certain studies lacking comprehensive coverage of magnetic field ranges [5] and omitting specific ferrofluids or Al_2O_3 [6].

An insightful study utilized the lattice Boltzmann method to analyze thermal management in a shell and tube heat exchanger using Fe_3O_4/water nanoliquid. This investigation assessed the influence of various parameters, such as the Rayleigh number, nanoparticle concentration, Hartmann number, magnetic field inclination angle, and thermal configuration of active tubes, on the flow structure and heat transfer properties. It was observed that heat transfer efficiency is inversely proportional to the Hartmann number, yet directly proportional to the inclination angle of the magnetic field [7]. In a pivotal study, the influence of non-uniform magnetic fields on the thermal efficiency of a cylindrical solar collector employing ferrofluid was investigated. It was discovered that an increase in the ferrofluid's volume fraction led to a significant enhancement in the collector's overall thermal efficiency. Remarkably, an efficiency increases of 48.54% was observed at a flow rate of 0.033 kg/s with a 1.0% volume fraction of ferrofluid. Moreover, at a lower flow velocity of 0.00415 kg/s and the same volume fraction, the maximum efficiency enhancement recorded was 26.8% [8]. Another research focused on the thermal-hydraulic parameters in laminar forced convection of aqueous magnetite ferrofluid within a rifled tube, under the influence of rotating magnetic field (RMF). Four different layouts were meticulously analyzed. The findings suggested that the combined application of a rifled tube and RMF offers hydrothermal advantages. The most noteworthy result was the attainment of a maximum performance evaluation criterion (PEC) value of 1.601 in RMF examples [9].

Further, a study examined the effects of magnetic field intensity on the convective heat transfer (CHT) characteristics of nanofluids containing cobalt-zinc ferrite nanoparticles. Results indicated that the CHT coefficient escalated in tandem with the increase in nanofluid concentration, reaching its apex at 0.2 weight percent. Additionally, an increment in magnetic field strength resulted in a 17% rise in the pressure drop rate [10]. An innovative approach was presented in a study focusing on accelerating the melting process of phase change materials (PCM) by integrating magnetic particles into liquid PCM. This method, involving forced convection, significantly expedited the solid PCM melting process. In an experimental setup featuring a side-heated cylinder, a 22.91% reduction in melting time was achieved at a rotation speed of 20 rev/min, particle fraction of 1.01 weight percent, and a heating temperature of 351°C [11]. However, a limitation of this study was the substitution of PCM for nanofluid. Additionally, an investigation proposed enhancing PCM melting through a convection intensity technique. This method entailed the movement of magnetic particles in liquid PCM between the heating element and the solid-liquid interface under forced convection. Experiments conducted in a bottom-heated cylinder demonstrated a 15.8% decrease in melting time at a temperature of 551°C. Concurrently, there was a notable 25.4% increase in the overall heat transfer coefficient at the interface between the heating surface and the solid-liquid phase.

A significant finding was reported in which a 10% relative variation in the prediction of the Nusselt number was observed [12]. However, this research utilized PCM rather than nano-ferrofluid, highlighting a gap in the application of such fluids in heat transfer enhancement. Further exploration in the field revealed a novel concept wherein mechanical energy is converted to electrical energy via ferrofluids. This process involves the ascent of air bubbles through induction coils, generating an electromotive force. Such a mechanism holds promise for non-contact sensor applications, monitoring of boiling two-phase flow in heat exchangers, and early detection of heat transfer deterioration, with the induced voltage being proportional to the air bubble's volume and velocity [13]. Another study delved into the natural convection and entropy generation in a micro-polar Multi-Walled Carbon Nano-Tube (MWCNT)-Fe_3O_4/water hybrid nanofluid, employing the finite element method (FEM). The research findings indicated that both the micro-rotation parameter and Hartmann number inversely affect natural convection and average Nusselt number, while the Bejan number increases with a reduced Rayleigh number. This study has practical implications for solar collectors, heat exchangers, and biomedical engineering, particularly in the context of blood flow [14]. In a related investigation, the heat transfer in serially connected PCM thermal battery units utilizing Al_2O_3-based nanofluid was analyzed. This study employed the Crank-Nicolson numerical method and incorporated the borehole heat exchanger concept, leading to insights into the transient thermal performance, mean temperature variations, and temperature profiles along storage tank depths and exits [15].

This research endeavors to scrutinize the flow and heat transfer enhancement of Fe_3O_4-distilled water in a tube subjected to a magnetic field. The objectives are as follows:

- To numerically analyze the influence of increased nanofluid concentration on the Nusselt number of the flow rate. This analysis will occur after determining the nanofluids' density, viscosity, specific heat, and thermal conductivity, with a particular focus on ferrofluid Fe_3O_4 at 0.5 weight percent.
- To examine the Y^+ gradient in relation to the number of magnets in the nanofluid, which will be calculated using dedicated software.
- To employ the Fluent program within ANSYS for simulating aspects of this phenomenon, thereby gaining deeper insights into the interplay of these factors in heat transfer processes.

2 Theoretical Analysis

This section delineates the fundamental equations employed to derive the results from the numerical analysis, highlighting the requisite software and configurations for ensuring accuracy and reliability in the findings.

2.1 The Energy Equation

The energy equation is resolved using ANSYS Fluent, as illustrated in Eq. (1).

$$\frac{\partial}{\partial t}\left(\rho\left(e+\frac{v^2}{2}\right)\right)+\nabla\cdot\left(\rho v\left(h+\frac{v^2}{2}\right)\right)=\nabla\cdot\left(k_{eff}\nabla T-\sum_j h_j\vec{J}_j+\dot{\tau}_{eff}\cdot\vec{v}\right)+S_h \tag{1}$$

where, the effective conductivity is denoted as k_{eff}, the turbulent conductivity is contingent on the chosen turbulence model, and $\vec{J}_j$ represents the species j dispersion transition. The right-hand side of the equation encompasses three principal terms addressing energy transfer due to conduction, species dispersion, and turbulent scattering, respectively. The term S_h integrates the rate of thermal aging stemming from chemical reactions, in addition to volumetric heat sources identified in the study. It is important to note that this reactive source does not exert an influence on the overall enthalpy state, as detailed under the section concerning energy sources due to reaction. For ideal gases, enthalpy h is defined as per Eq. (2), aligning with the classical thermodynamic principles.

$$h=\sum_j Y_j h_j \tag{2}$$

In the analysis of incompressible materials, the energy equation incorporates the contribution from pressure work, as delineated in Eq. (3).

$$h=\sum_j Y_j h_j+\frac{p}{\rho} \tag{3}$$

where, Y_j represents the mass fraction of species j, and the sensible heat of the species h_j, defined in Eq. (4), pertains exclusively to enthalpy changes attributable to specific heat.

$$h_j=\int_{T_{ref}}^{T} c_{p,j}dT \tag{4}$$

The choice of solver and models dictates the reference temperature (T_{ref}) employed in the sensible enthalpy calculations. Excluding Probability Density Function (PDF) models, where T_{ref} is an input parameter specified by the user for each species, and is universally set at 298.15 K for the density-based solver. In cases involving species transport with reactions, T_{ref} is user-specified; however, for the viscositybased solution, it defaults to 0.

In situations involving materials that are both compressible and incompressible, the internal energy equation is uniformly articulated, as shown in Eq. (5).

$$e=h-\frac{p_{op}+p}{\rho} \tag{5}$$

where, P and p_{op} denote the check pressure and operating pressure, respectively. The accurate definition of enthalpy and internal energy for an incompressible ideal gas necessitates the application of Eq. (6).

$$h=c_v T+\frac{p_{abs}}{\rho}=c_v T+R_g T+\frac{p}{\rho}=c_p T+\frac{p}{\rho} \tag{6}$$

2.2 Equations for Conservation of Momentum

The methodology employed in this research incorporates the fundamental equations governing the conservation of momentum, essential for 2D axisymmetric computations. These equations are represented as Eqs. (7) and (8).

$$\begin{aligned}\frac{\partial}{\partial t}\left(\rho v_x\right)+\frac{1}{r}\frac{\partial}{\partial x}\left(r\rho v_x v_x\right)+\frac{1}{r}\frac{\partial}{\partial r}\left(r\rho v_r v_x\right)=&-\frac{\partial p}{\partial x}\\&+\frac{1}{r}\frac{\partial}{\partial x}\left[r\mu\left(2\frac{\partial v_x}{\partial x}-\frac{2}{3}(\nabla\cdot\vec{v})\right)\right]\\&+\frac{1}{r}\frac{\partial}{\partial r}\left[r\mu\left(\frac{\partial v_x}{\partial r}+\frac{\partial v_r}{\partial x}\right)\right]+F_x\end{aligned} \tag{7}$$

and

$$\begin{aligned}\frac{\partial}{\partial t}\left(\rho v_r\right)+\frac{1}{r}\frac{\partial}{\partial x}\left(r\rho v_x v_r\right)+\frac{1}{r}\frac{\partial}{\partial r}\left(r\rho v_r v_r\right)=&-\frac{\partial p}{\partial r}\\&+\frac{1}{r}\frac{\partial}{\partial x}\left[r\mu\left(\frac{\partial v_r}{\partial x}+\frac{\partial v_x}{\partial r}\right)\right]\\&+\frac{1}{r}\frac{\partial}{\partial r}\left[r\mu\left(2\frac{\partial v_r}{\partial r}-\frac{2}{3}(\nabla\cdot\vec{v})\right)\right]\\&-2\mu\frac{v_r}{r^2}+\frac{2}{3}\frac{\mu}{r}(\nabla\cdot\vec{v})+\rho\frac{v_z^2}{r}+F_r\end{aligned} \tag{8}$$

where,

$$\nabla\cdot\vec{v}=\frac{\partial v_x}{\partial x}+\frac{\partial v_r}{\partial r}+\frac{v_r}{r} \tag{9}$$

And v_z is the swirl velocity.

2.3 System Geometry

In the configuration of the experimental model, the inner diameter of the flow channel was established at 25.4 mm, and the total length of the tube extended to 210 mm. The positioning of the magnets along the tube's surface was meticulously designed, with their locations being uniformly distributed. Each magnet spanned a width of 10 mm and was placed at intervals of 45 mm. This precise arrangement facilitated the uniform distribution of the magnetic field along the tube's length. The tube's outer layer represents the heat sources exposed to the wall. Figure 1 illustrates the geometry of the model.

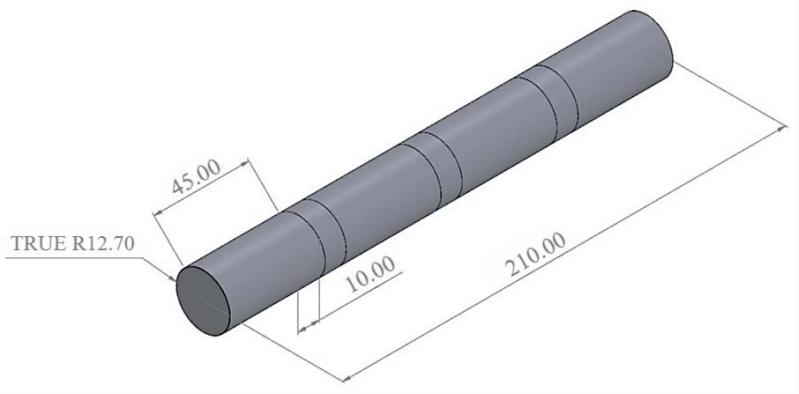

Figure 1. Geometry of the model

2.4 Mesh Generation and Boundary Conditions

In Computational Fluid Dynamics (CFD) simulations, conducting a mesh independence analysis is imperative to ensure that the results are not significantly influenced by the chosen mesh size. The selection of mesh element size is a critical factor that balances the accuracy and computational efficiency of the simulation. Ideally, the mesh's fineness must be sufficient to accurately capture essential flow characteristics and gradients, while avoiding excessive refinement that could lead to prohibitive computational costs.

The objective of mesh independence research is to ascertain the impact of mesh resolution on the solution. This is achieved by conducting simulations with various mesh sizes and comparing the results. Key evaluation criteria include the stability of the solutions, consistency in flow field patterns, and fulfillment of convergence criteria. The strategy involves starting with a coarser mesh and progressively refining it, comparing outcomes with each level of refinement until further refinement ceases to yield significant improvements. For this study, unstructured tetrahedral grids were utilized due to their effectiveness in handling complex geometries. ANSYS software facilitated the generation of three-dimensional models and solid geometry meshes with minimal user input. The total number of cells generated for this investigation was 1,451,380. Mesh independence was established by observing the stabilization of output results and setting the element size at 0.0005 m, ensuring the accuracy and reliability of the results. Table 1 presents the data from the mesh independence analysis.

Table 1. Mesh independence analysis

Case	Node	Element	Max. Temperature (K)	Outlet Temperature (K)	Pressure Difference (Pa)
1	634212	523421	335.812	346.31	0.0455
2	1063643	974323	331.493	343.99	0.0394
3	1304363	1243667	329.081	343.81	0.0379
4	1505772	1451380	329.074	343.79	0.0378

In an ideal computational environment, residuals would diminish to zero as a simulation converges. However, in practical scenarios using real computers, residuals decay to a minimal value and then stabilize. This stabilization indicates the convergence of the simulation within the computational limits. The fluid flow conditions, as per the CFD approach, are iteratively adjusted until satisfactory convergence is achieved. Convergence is deemed to have occurred when the residuals, indicative of the difference between successive iterations of a variable, fall below a predetermined threshold. Typically, residuals are scaled by the largest absolute residual observed in the initial iterations. In this study, convergence was determined when the residuals for all flow conditions fell below a threshold of 10^{-6}.

At the inlet, three distinct entrance velocities (0.05, 0.1, and 0.5 m/s) were employed, representing the introduction of nanomaterial at 300 K. This range of velocities was chosen based on their prevalence in practical applications, as per available market data. Three scenarios were simulated with varying magnet configurations: initially with the middle magnet activated, followed by activation of the first and third magnets, and ultimately with all three magnets operational. At the outlet, an exit pressure of 0 Pa was maintained, with the heat surfaces held at a constant temperature of 350 K. This exit temperature was selected to enable clear observation of the cooling process while avoiding temperatures that could induce phase transformation in the fluid. Magnetic flux densities of one, two, and three Teslas were analyzed to assess their impact on the flow and heat transfer characteristics of the nanofluid.

3 Results and Discussion

This section is dedicated to a comprehensive examination and interpretation of the outcomes derived from the simulation program. The analysis is bifurcated into two primary focuses: the assessment of Y^+ values under various parameters and the variations observed in the Nusselt numbers.

3.1 Analysis of the Nusselt Number Based on Case Parameters

The categorization of instances was conducted based on the fluid's entrance velocity. It was observed, as depicted in Figure 2, that the Nusselt number escalates with an increase in magnetic field strength. This trend suggests that the induction of turbulence in the fluid enhances its thermal absorption capacity. At a magnetic field influence of three Teslas, the Nusselt number attained a peak value of 75.8, marking the highest figure in comparison to other magnetic field strengths.

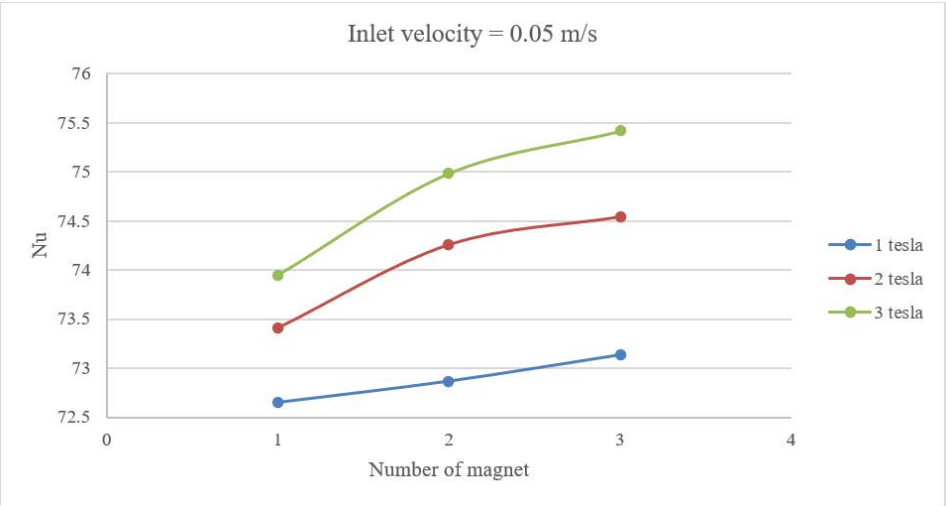

Figure 2. Nusselt number gradient at 0.05 m/s inlet velocity with varying numbers of magnets

Turbulence, a state of fluid flow, is characterized by its erratic and unpredictable motions. It manifests in complex, multidimensional patterns of fluid particle movement, leading to the formation of vortices, eddies, and fluctuations in pressure and velocity. The onset of turbulence, marked by the transition from smooth, laminar flow to chaotic motion,

significantly influences heat transfer, mixing efficiency, and overall fluid dynamics. Its impact is profound in various engineering applications, dictating the effectiveness of heat transfer processes.

When the flow velocity was increased to 0.1 m/s, the Nusselt number peaked at 128.7 under the influence of a magnetic field of 3 Teslas, as shown in Figure 3.

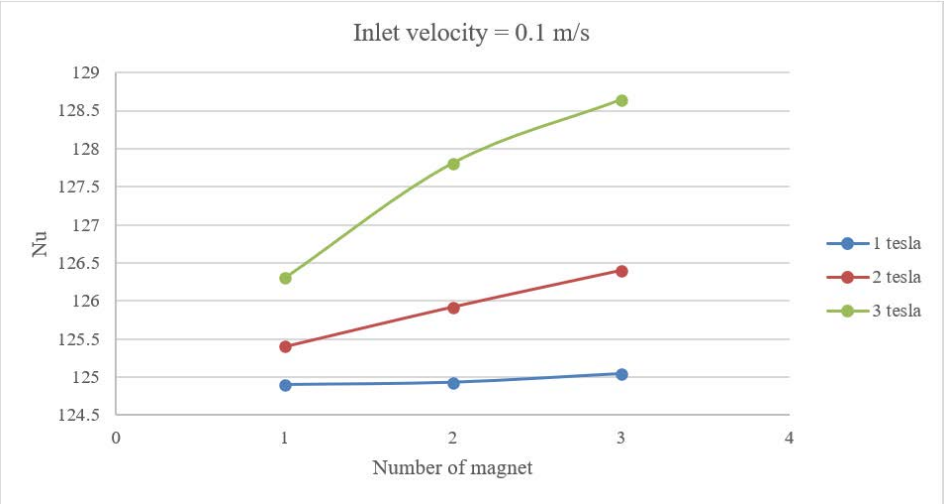

Figure 3. Nusselt number gradient at 0.1 m/s inlet velocity with varying numbers of magnets

At a higher flow velocity of 0.5 m/s, a notable decrease in the Nusselt number to 3 was observed upon the introduction of magnets. This decrease can be attributed to the rapid flow velocity, which does not allow sufficient time for heat transfer from the tube to the fluid.

The augmentation in fluid momentum, associated with increasing inlet velocity, leads to a diminution of the hydrodynamic boundary layer. This reduction accelerates the flow over the surface, potentially curtailing the duration required for CHT. The hydrodynamic boundary layer plays a pivotal role in heat transport, with its thickness inversely proportional to velocity, thereby influencing convective heat transmission. A decrease in the hydrodynamic boundary layer thickness is correlated with a reduction in the Nusselt number, which is a measure of the ratio of convective to conductive heat transfer. The thermal boundary layer's behaviour is governed by two primary factors: the flow rate and the applied magnetic field. At elevated velocities, the thermal boundary layer becomes thinner, potentially abbreviating the period of thermal energy exchange. Additionally, the Lorentz force, which influences fluid flow in the presence of a magnetic field, significantly impacts the thermal boundary layer. The temperature distribution alterations, resultant from the interaction between the flowing fluid and the magnetic field, are reflected in the changes observed in the Nusselt number.

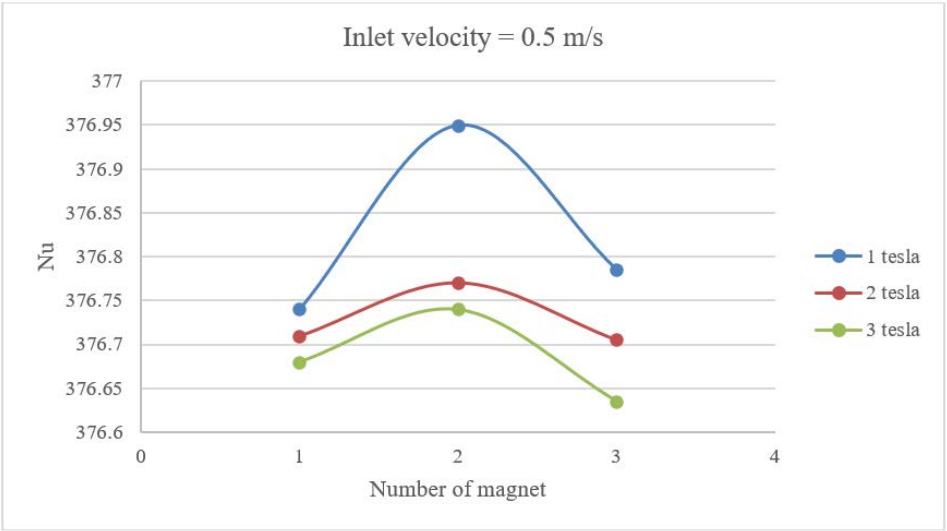

Figure 4. Nusselt number gradient at 0.5 m/s inlet velocity with varying numbers of magnets

The interplay between the hydrodynamic and thermal boundary layers is of utmost importance. While an increase in velocity leads to a decrease in the Nusselt number, the magnetic field can counterbalance this effect by modifying the fluid's temperature distribution. There might exist an optimal velocity for maximizing heat transfer efficiency. Beyond this velocity, a further decrease in the hydrodynamic boundary layer thickness could account for the observed dip in the Nusselt number. Figure 4 demonstrates the gradient of the Nusselt number at an inlet velocity of 0.5 m/s with varying numbers of magnets.

3.2 Analysis of Y^+ Based on Case Parameters

In this segment of the study, the categorization of instances was done in accordance with the fluid's entrance velocity. It has been discerned, as showcased in Figure 5, that the Y^+ value escalates with an increase in magnetic field strength. This trend indicates that turbulence induction in the fluid enhances its capacity for temperature transfer. At a magnetic field strength of three Teslas, the Y^+ value peaked at 0.84, representing the highest value attained in comparison to other magnetic field intensities. Figure 6 presents the Y^+ gradient with the number of magnets at an inlet velocity of 0.1 m/s.

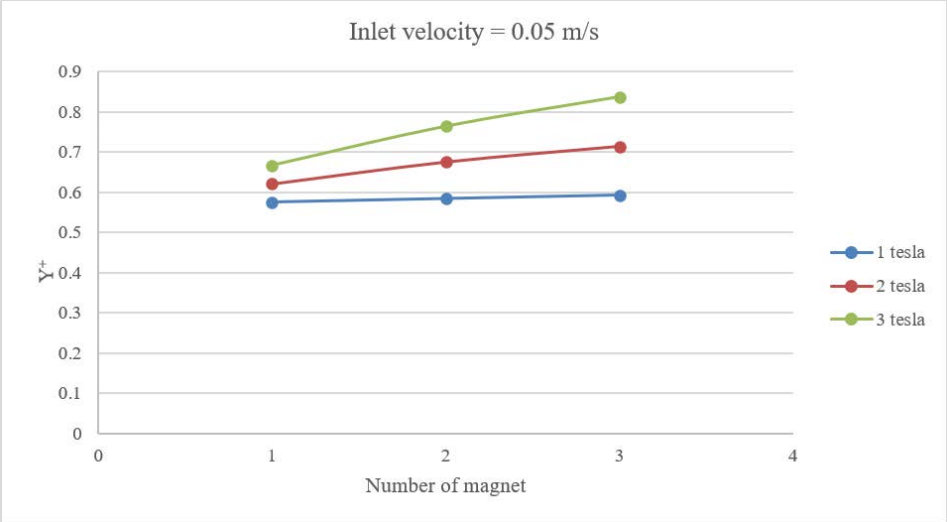

Figure 5. Y^+ gradient at an inlet velocity of 0.05 m/s with varying numbers of magnets

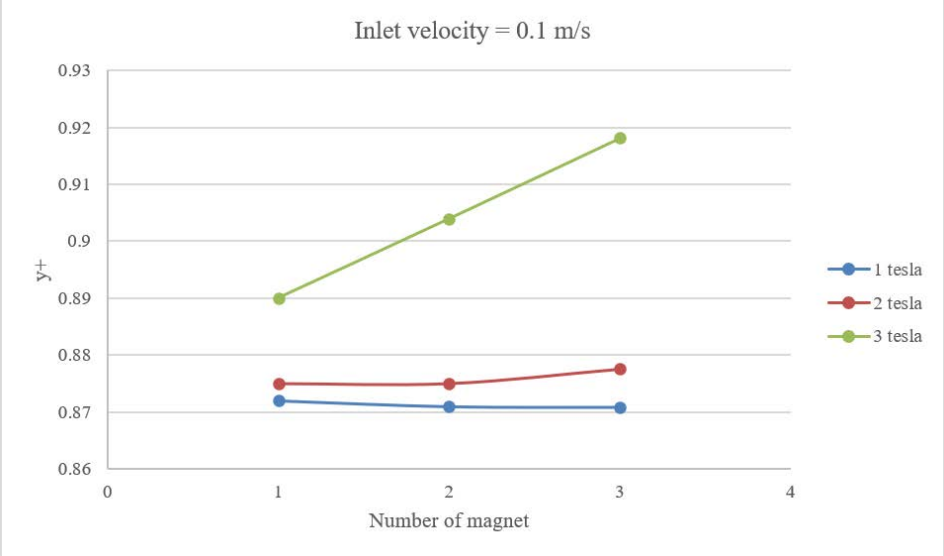

Figure 6. Y^+ gradient at an inlet velocity of 0.1 m/s with varying numbers of magnets

In scenarios where the flow velocity was established at 0.1 m/s, the Y^+ value was observed to reach 0.915 under the influence of a magnetic field of 3 Teslas.

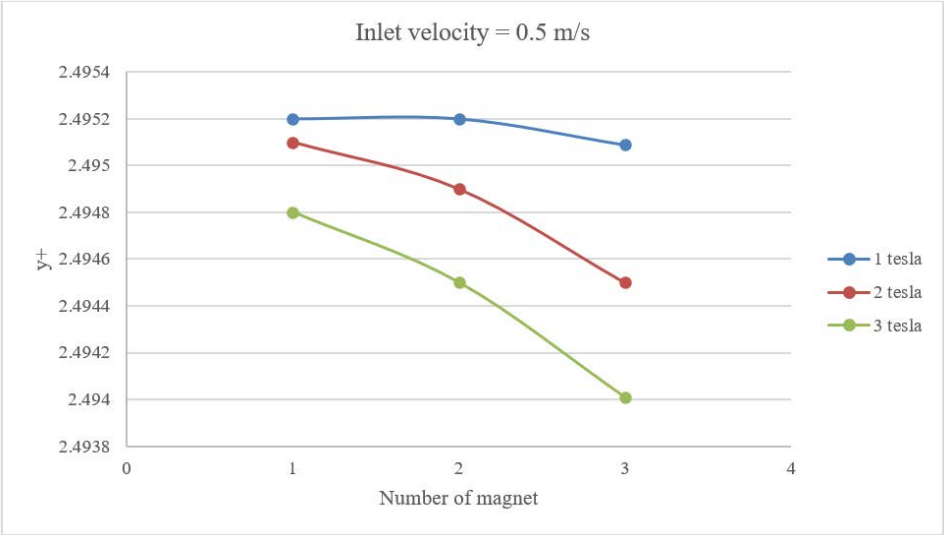

Figure 7. Y^+ gradient at an inlet velocity of 0.5 m/s with varying numbers of magnets

As illustrated in Figure 7, the behavior of Y^+ under a flow velocity of 0.5 m/s was observed. The arrival of magnets resulted in a reduction of Y^+ to 3. This phenomenon can be attributed to the accelerated flow velocity, which curtails the duration available for heat transfer from the tube to the fluid.

The Y^+ parameter is a dimensionless measure that denotes the distance between the wall and the first grid node in the near-wall zone. It is intrinsically linked to wall shear stress and serves as an indicator of the adequacy of the near-wall mesh in turbulence modeling. Higher Y^+ values suggest a coarser near-wall mesh, indicating that the initial grid node is positioned further from the wall. This positioning is associated with a region adjacent to the wall where turbulence models may not accurately represent the flow mechanics. Conventionally, Y^+ values below 5 are aligned with a "wall-function" approach, deemed suitable for resolving flows near the wall. The observation that Y^+ values increase with the intensity of the magnetic field suggests alterations in near-wall flow behavior induced by the magnetic field. This field can modulate turbulence characteristics, altering fluid flow patterns and consequently affecting turbulence intensity.

The influence of the magnetic field on the fluid results in variations in the velocity profile near the wall, which in turn impacts the Y^+ values. Enhanced turbulence promotes heat transfer by facilitating fluid mixing near the wall, typically leading to increased CHT. However, changes in turbulence characteristics, as reflected in Y^+ values, could significantly influence the heat transfer process. Furthermore, Y^+ plays a role in shaping both the hydrodynamic and thermal boundary layers. Alterations in Y^+ values due to the magnetic field can modify the thickness and characteristics of the thermal boundary layer, thereby impacting the rate of CHT. This interplay between the magnetic field, turbulence, and heat transfer underscores the complexity of the fluid dynamics in the presence of magnetic fields.

3.3 Comparison with Previous Research

In this study, the geometrical setup was compared with existing research involving ferromagnetic materials to validate the accuracy of the simulation software. The design incorporated channels at both the entrance and the outlet, each measuring 2 mm in width and 500 μm in depth. A circular chamber, with a diameter (D) of 6 mm and a depth (H) of 500 μm, was fabricated using a laser engraving technique on a transparent double-sided adhesive tape with a thickness of 500 μm. This method aligns with established fabrication practices in the field (source, brand of the tape).

To investigate the impact of the magnetic field, a neodymium–iron–boron (NdFeB) permanent magnet cube, grade N42 and measuring 3.2 mm^3, was strategically positioned adjacent to the chamber. A diluted water-based ferrofluid (EMG707, Ferrotec), categorized as a paramagnetic fluid, was introduced into the setup. Prior studies had measured and reported the magnetic field strength of the permanent magnet as a function of distance from the magnet, providing a basis for comparison. The flow rate in these experiments ranged from 50 to 400 μL/min [16].

Figure 8 illustrates the outlet temperature at various flow rates. The exit temperatures obtained from the simulations were compared with the variations in flow rate, following a model design and configuration necessary for accurate comparative analysis. The results exhibited a marginal deviation, with an error rate of up to 10% when compared to the outcomes of the prior research. The error percentage was calculated by dividing the results from the previous study by those obtained in the current work and multiplying by 100%.

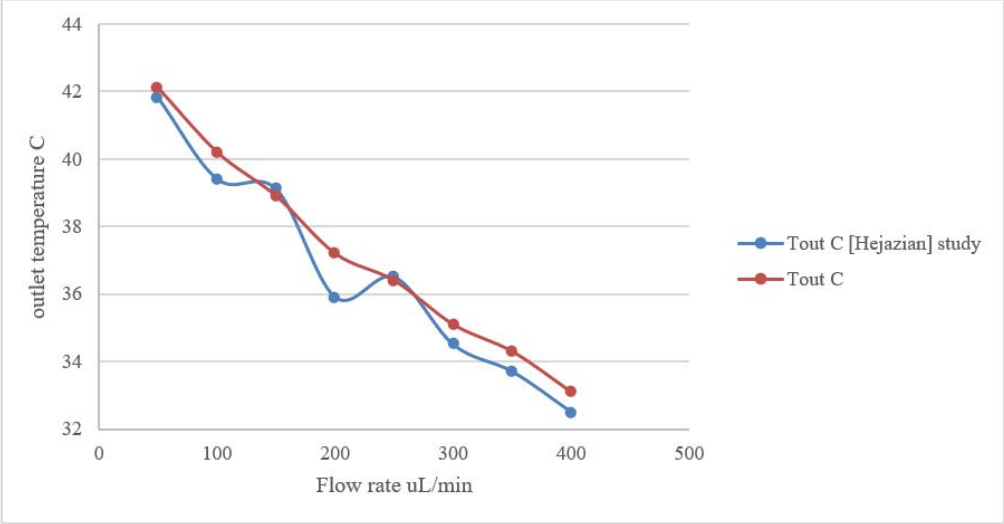

Figure 8. Outlet temperature at C at various flow rates

4 Conclusions and Recommendations

The findings of this study provide intriguing insights into the interaction between magnetic fields and fluid dynamics. Contrary to initial predictions, it has been observed that the presence of a magnetic field indeed augments turbulence near the wall. This phenomenon is attributed to the generation of Lorentz force by the magnetic fields, which alters the flow dynamics, leading to modifications in the conventional structure of the boundary layer. Analytical results derived from the Nusselt numbers indicate that a stronger magnetic field unexpectedly enhances heat transfer. This outcome deviates from prior assumptions and underscores the influential role of the magnetic field in heat transfer processes. The interaction between the fluid and the magnet has been shown to impact both the hydrodynamic and thermal boundary layers. Theoretical analyses suggest that this interaction not only promotes mixing but also inhibits the formation of thermal boundary layers, thereby facilitating the enhancement of CHT.

From the investigations conducted in this study, the following conclusions are drawn:

- The increase in magnetic flux value impedes the flow and amplifies channel vortices by influencing the movement of the fluid's magnetic material particles, which align with the direction of the flux. These magnetic material particles, being ferromagnetic or ferrimagnetic, exhibit magnetic moments and are responsive to magnetic fields. The dynamic behavior of ferrofluids, triggered by an applied magnetic field, leads to the motion of these magnetic particles. This motion is reflective of the inherent behavior of ferrofluids, where magnetic nanoparticles suspended in the fluid alter their movement in response to magnetic fields. The observation of magnetic material particles' motion within the ferrofluid, particularly under external magnetic fields, holds significant practical implications, especially in systems requiring precise fluid dynamic control. The potential of ferrofluids, augmented by the responsiveness of magnetic particles to magnetic fields, opens new avenues in magneto-rheological applications and targeted drug delivery systems.
- A positive correlation between the Nusselt number and magnetic field strength was noted, indicating that increased turbulence, induced by the magnetic field, enhances the fluid's heat transfer capabilities. The complex interplay of magnetic fields, turbulence, and heat transfer underscores the significance of understanding the transient effects of magnetic fields on both hydrodynamic and thermal boundary layers for comprehensive insight into these phenomena.
- The study reveals a direct relationship between Y^+ values and magnetic field strength, suggesting that turbulence assists in temperature transfer within the fluid. Variations in Y^+ values, indicative of enhanced turbulence levels, are closely associated with stronger magnetic fields. This turbulence, particularly near the wall, may be responsible for the observed changes in Y^+ readings. The alterations in Nusselt numbers as a function of magnetic field strength provide compelling evidence of the impact of this parameter on heat transfer processes.

In light of the findings presented, the following recommendations are proposed to guide future research and practical applications:

- Given the established impact of magnetic fields on heat transfer and fluid dynamics, further exploration into magnetohydrodynamic processes is advised. It is essential to examine the interactions of various fluid compositions with magnetic fields, with a particular emphasis on the variations in magnetic particle concentration. This investigation will enhance the understanding of magnetohydrodynamic phenomena and their implications for different fluid types.

- Due to the transient nature of the effects observed, particularly with fluctuating magnetic field strengths, additional research is imperative. Future studies should concentrate on understanding the behavior of fluid flow and heat transfer under dynamic magnetic fields over time. This focus is crucial for comprehending the temporal dynamics of these processes.
- The use of numerical models to simulate fluid flow and heat transfer in the presence of magnetic fields is recommended to supplement experimental data. This approach will deepen the comprehension of the underlying physics and augment the predictive accuracy of simulation models. Such numerical modeling will provide valuable insights into the mechanisms governing magnetically influenced fluid dynamics and heat transfer.

Data Availability

The data used to support the findings of this study are available from the corresponding author upon request.

Conflicts of Interest

The authors declare no conflict of interest.

References

[1] M. Ghasemian, Z. N. Ashrafi, M. Goharkhah, and M. Ashjaee, "Heat transfer characteristics of Fe_3O_4 ferrofluid flowing in a mini channel under constant and alternating magnetic fields," *J. Magn. Magn. Mater.*, vol. 381, pp. 158–167, 2015. https://doi.org/10.1016/j.jmmm.2014.12.078

[2] A. Shahsavar, M. Saghafian, M. R. Salimpour, and M. B. Shafii, "Experimental investigation on laminar forced CHT of ferrofluid loaded with carbon nanotubes under constant and alternating magnetic fields," *Exp. Therm. Fluid Sci.*, vol. 76, pp. 1–11, 2016. https://doi.org/10.1016/j.expthermflusci.2016.03.010

[3] Z. Narankhishig, J. Ham, H. Lee, and H. Cho, "Convective heat transfer characteristics of nanofluids including the magnetic effect on heat transfer enhancement - A review," *Appl. Therm. Eng.*, vol. 193, p. 116987, 2021. https://doi.org/10.1016/j.applthermaleng.2021.116987

[4] X. Zhang and Y. Zhang, "Heat transfer and flow characteristics of Fe_3O_4-Water nanofluids under magnetic excitation," *Int. J. Therm. Sci.*, vol. 163, p. 106826, 2021. https://doi.org/10.1016/j.ijthermalsci.2020.106826

[5] X. Zhang and Y. Zhang, "Experimental study on enhanced heat transfer and flow performance of magnetic nanofluids under alternating magnetic field," *Int. J. Therm. Sci.*, vol. 164, p. 106897, 2021. https://doi.org/10.1016/j.ijthermalsci.2021.106897

[6] Y. Sheikhnejad, R. Hosseini, and M. Saffar-Avval, "Effect of different magnetic field distributions on laminar ferroconvection heat transfer in horizontal tube," *J. Magn. Magn. Mater.*, vol. 389, pp. 136–143, 2015. https://doi.org/10.1016/j.jmmm.2015.04.029

[7] Y. Ma, R. Mohebbic, M. M. Rashidid, Z. Yang, and M. Sheremetf, "Nanoliquid thermal convection in I-shaped multiple-pipe heat exchanger under magnetic field influence," *Physica A*, vol. 550, p. 124028, 2020. https://doi.org/10.1016/j.physa.2019.124028

[8] E. Shojaeizadeh, F. Veysi, H. Habibi, K. Goodarzi, and M. Habibi, "Thermal efficiency investigation of a ferrofluid-based cylindrical solar collector with a helical pipe receiver under the effect of magnetic field," *Renew. Energy*, vol. 176, pp. 198–213, 2021. https://doi.org/10.1016/j.renene.2021.05.049

[9] S. Rasaee, A. Shahsavar, and K. Niazi, "Experimental assessment on convection heat transfer characteristics of aqueous magnetite ferrofluid in a rifled tube under a rotating magnetic field," *Int. Commun. Heat Mass Transfer*, vol. 129, p. 105673, 2021. https://doi.org/10.1016/j.icheatmasstransfer.2021.105673

[10] A. Lee, Y. Jeon, V. Chinnasamy, and H. Cho, "Investigation of forced CHT with magnetic field effect on water/ethylene glycol-cobalt zinc ferrite nanofluid," *Int. Commun. Heat Mass Transfer*, vol. 128, p. 105647, 2021. https://doi.org/10.1016/j.icheatmasstransfer.2021.105647

[11] Y. Fan, M. Yu, C. Zhang, L. Jiang, X. Zhang, and Y. Zhao, "Melting performance enhancement of PCM with magnetic particles under rotating magnetic field," *J. Energy Storage*, vol. 38, p. 102540, 2021. https://doi.org/10.1016/j.est.2021.102540

[12] Y. Fan, C. Zhang, M. Yu, X. Zhang, and Y. Zhao, "Performance enhancement of latent thermal energy system under alternating magnetic field," *Appl. Therm. Eng.*, vol. 188, p. 116586, 2021. https://doi.org/10.1016/j.applthermaleng.2021.116586

[13] F. Jiao, Q. Li, and Y. He, "Electromotive force induced by the moving non-magnetic phase in ferrofluids," *Sens. Actuators A Phys.*, vol. 317, p. 112472, 2021. https://doi.org/10.1016/j.sna.2020.112472

[14] M. M. Rahman, A. J. Chamkha, Y. Elmasry, I. Ullah, A. Pasha, M. S. Sadeghi, and A. M. Galal, "The heat transfer behavior of MHD micro-polar MWCNT-Fe_3O_4/water hybrid nanofluid in an inclined $\perp$ shaped cavity with semi-circular heat source inside," *Case Stud. Therm. Eng.*, vol. 38, p. 102316, 2022. https://doi.org/10.1016/j.csite.2022.102316

[15] S. A. Asiri, E. M. Salilih, K. M. Alfawaz, A. F. Alogla, S. M. Sajadi, and O. K. Nusier, "Transient heat transfer analysis of serially connected array of phase change material in the thermal battery units with Al_2O_3 working nano fluids," *J. Energy Storage*, vol. 53, p. 105184, 2022. https://doi.org/10.1016/j.est.2022.105184

[16] M. Hejazian and N. Nguyen, "Magnetofluidics for manipulation of convective heat transfer," *Int. Commun. Heat Mass Transfer*, vol. 81, pp. 149–154, 2017. https://doi.org/10.1016/j.icheatmasstransfer.2016.12.017